Hindawi
Wireless Communications and Mobile Computing
Volume 2021, Article ID 1981388, 12 pages
https://doi.org/10.1155/2021/1981388

Research Article

Evaluation and Prediction of COVID-19 Prevention and Control Strategy Based on the SEIR-AQ Infectious Disease Model

Yue Yu, Yuxing Zhou, Xiangzhong Meng, Wenfei Li, Yang Xu, Manfeng Hu, and Jingxiang Zhang

School of Science, Jiangnan University, 1800 Lihu Avenue, Wuxi, Jiangsu 214122, China

Correspondence should be addressed to Jingxiang Zhang; zhangjingxiang@jiangnan.edu.cn

Received 8 May 2021; Revised 23 May 2021; Accepted 31 May 2021; Published 11 June 2021

Academic Editor: Shan Zhong

Based on the SEIR model, which takes into account prevention and control measures, prevention and control awareness, and economic level and medical level indicators, this paper proposes an infectious disease model of "susceptible-exposed-infected-removed-asymptomatic-isolated" (short for SEIR-AQ) to assess and predict the development of the COVID-19 pandemic with different prevention and control strategies. The kinetic parameters of the SEIR-AQ model were obtained by fitting, and the parameters of the SEIR-AQ model were solved through the Euler method. Furthermore, the effects of different countries' prevention and control strategies on the number of infections, the proportion of isolation, the number of deaths, and the number of recoveries were also simulated. The theoretical analysis showed that measures such as isolation for prevention and control and medical tracking isolation had a significant inhibitory effect on the development of the COVID-19 pandemic, among which stratified treatment and enhanced awareness played a key role in the rapid regression of the peak of COVID-19-infected patients. *Conclusion of the Simulation*. The SEIR-AQ model can be used to evaluate the development status of the COVID-19 epidemic and has some theoretical value for the prediction of COVID-19.

1. Introduction

Coronavirus disease 2019 is a lung disease caused by SARS-CoV-2, which is highly lethal and infectious [1]. Some scholars have clinically analyzed the causes of death in patients with confirmed COVID-19 [2] and identified factors associated with the death of patients with COVID-19 pneumonia caused by the novel coronavirus SARS-CoV-2 [3]. With 130566186 cumulative diagnoses and 2842363 cumulative deaths worldwide as of April 4, 2021, COVID-19 not only impacted the global economy but also deeply affected the governance of all countries in the world.

For COVID-19 epidemic prediction, most scholars used the classical SIR and SEIR models proposed by Beretta and Takeuchi [4] and Cooke and van den Driessche [5] to infer the COVID-19 peak time and maximum number of confirmed cases based on the existing data. Yu et al. [6] evaluated and predicted COVID-19 based on a SIR model with time-varying parameters to obtain expected inflection points and maximum number of confirmed cases. Wei et al. [7] and Geng et al. [8] studied the effect of prevention and control isolation measures on the development trend of the COVID-19 epidemic based on the SEIR model and concluded that strict prevention and control isolation measures can slow down the development trend of the COVID-19 epidemic. Wang et al. [9] established the SEIADR model by introducing asymptomatic infected individuals on the traditional SEIR model. Also, they predicted the development of the COVID-19 epidemic in Hubei Province, which had better fitting effect compared with the SEIR model. Shao et al. [10] used the classical SEIR model to conduct a predictive analysis of COVID-19 in Shandong Province and Korea, comparing the impact of control measures on the spread of COVID-19. Li et al. [11] fitted the COVID-19 regeneration coefficient (R_0) curve based on the SEIR model to predict and analyze the development trend of the COVID-19 epidemic in Hubei Province, China, America, India, Italy, and Iran and also predicted that the spread of the epidemic in Hubei Province

would be better controlled compared with that of foreign countries. Lin [12], Chen et al. [13], and Ansumali et al. [14] introduced asymptomatic infected individuals based on the SEIR model, which led to a significant improvement in the fitting and prediction performance of the SEIR model. Ivorra et al. [15] developed the θ-SEIHRD model, where asymptomatic infected patients and medical conditions were taken into account, which could predict hospital bed demand more accurately. Pai et al. [16] improved the SEIR model by integrating government control policies, public health, and other factors to analyze the impact on the development trend of COVID-19 in India.

Although the above-mentioned studies have achieved certain effects, they only consider the latent infectious capacity of COVID-19-infected people, the infectious capacity of asymptomatic patients, prevention and quarantine measures, etc. In fact, many other factors including different medical levels, economic levels, and prevention and control awareness also have a great impact on the transmission of COVID-19. Therefore, based on the SEIR model, we divided susceptible people, contacts, and infected people into isolated and exposed states and then introduced hospitalized patients and asymptomatic patients as well as indicators such as prevention and control measures, prevention and control awareness, economic level, and medical level to construct a more interpretive SEIR-AQ paradigm. The development trend of COVID-19 at different levels was simulated by adjusting the parameters of prevention and control measures, prevention and control awareness, economic level, and medical level.

2. Establishment of the SEIR-AQ Model

The traditional SEIR model divides the population into susceptible people (S), contacts (E), infected people (I), and recovered people (R). However, the SEIR-AQ paradigm adds isolation of susceptible people (S_q), isolation of contacts (E_q), isolation of infected people (I_q), asymptomatic patients (A), and hospitalized patients (H). Now, according to the proportion of b_1, b_2, and b_3, we converted the isolated infected people, unisolated infected people, and asymptomatic patients into hospitalized patients H. The SEIR-AQ paradigm assumes that the infected and quarantined people are not infectious during the isolation period, and the infected people are immune to cure. The parameter υ is the ratio of the transmission capacity of the unisolated contacts E to the unisolated infected people I, and the parameter θ is the ratio of the transmission capacity of the asymptomatic patients A to the unisolated infected people I. Therefore, the SEIR-AQ paradigm in this paper is more interpretive and adaptable. The warehouse conversion relationship of the SEIR-AQ paradigm is shown in Figure 1.

q, β, c, and ρ are the isolation ratio, the infection probability, the contact rate, and the effective contact coefficient, respectively, and ρc is the effective contact rate. The conversion rate from unisolated susceptible people (S) to isolation of S_q, E_q, and unisolated contacts (E) is $\rho cq(1-\beta)$, $\rho cq\beta$, and $\rho c\beta(1-q)$, respectively. At the same time, considering the impact of unisolated infected people (I), A, and E on susceptible populations, there is also isolation of S_q that is retransformed into S at a rate of λ. The natural death rate of S is η. Therefore, the governing equation for the number of susceptible people is

$$\frac{dS}{dt} = -[\rho c\beta + \rho cq(1-\beta)]S(I + \theta A + \upsilon \mathrm{E}) + \lambda \mathrm{S}_q - \eta S. \quad (1)$$

λ is the quarantine release rate, taking $\lambda = 1/14$ (the quarantine duration is 14 days).

The SEIR-AQ model considers different prevention and control measures, prevention and control awareness, economic level, and medical level:

$$\begin{cases} \dfrac{dS}{dt} = -[\rho c\beta + \rho cq(1-\beta)]S(I + \theta A + \upsilon E) + \lambda S_q - \eta S, \\ \dfrac{dE}{dt} = \rho c\beta(1-q)S(I + \theta A + \upsilon E) - (\sigma_1 + \sigma_2 + \sigma_3 + \eta)E, \\ \dfrac{dI}{dt} = -(b_1 + r_1 + \alpha_1)I + \sigma_1 eE + \delta_1 eE_q + p_1 A, \\ \dfrac{dA}{dt} = -(p_1 + p_2 + b_2 + r_2 + \alpha_2)A + \sigma_2(1-e)E + \delta_2(1-e)E_q, \\ \dfrac{dS_q}{dt} = \rho cq(1-\beta)S(I + \theta A + \upsilon E) - (\lambda + \eta)S_q, \\ \dfrac{dE_q}{dt} = \rho c\beta qS(I + \theta A + \upsilon E) - (\delta_1 + \delta_2 + \delta_3 + \eta)E_q, \\ \dfrac{dI_q}{dt} = -(b_3 + r_3 + \alpha_3)I_q + \sigma_3 eE + \delta_3 eE_q + p_2 A, \\ \dfrac{dH}{dt} = b_1 I + b_2 A + b_3 I_q - (r_4 + \alpha_4)H, \\ \dfrac{dR}{dt} = \mu_1 r_1 I + \mu_2 r_2 A + \mu_3 r_3 I_q + \mu_4 r_4 H - \eta R. \end{cases} \quad (2)$$

σ_1, σ_2, and σ_3 are the rates of conversion of E to I, A, and I_q, respectively, taking $\sigma_1 = \sigma_2 = \sigma_3 = 7$ (the incubation period is 7 days); α_1, α_2, α_3, and α_4 are the death rates of I, A, I_q, and H; δ_1, δ_2, and δ_3 are the rates of isolation of E_q to I, A, and I_q, respectively; p_1 and p_2 are the rates at which A turns into I and I_q; r_1, r_2, r_3, and r_4 are the recovery rate of I, A, I_q, and H; μ_1, μ_2, μ_3, and μ_4 are the coefficient of the recovery rate of I, A, I_q, and H; and e is the probability that the infected people have symptoms.

In fact, I_q will be immediately sent to a designated hospital for isolation and treatment during the COVID-19 epidemic; thus, I_q will all be converted into H in this model based on the SEIR-AQ model paradigm. Considering that the asymptomatic patients would not be taken to the hospital until any symptom was shown, we removed the asymptomatic patients into the relationship between the hospitalized patients and the infected people. E_q, if confirmed, will be directly sent to the hospital and converted into H. Therefore, the relationship that E_q is converted to I is removed. Based on

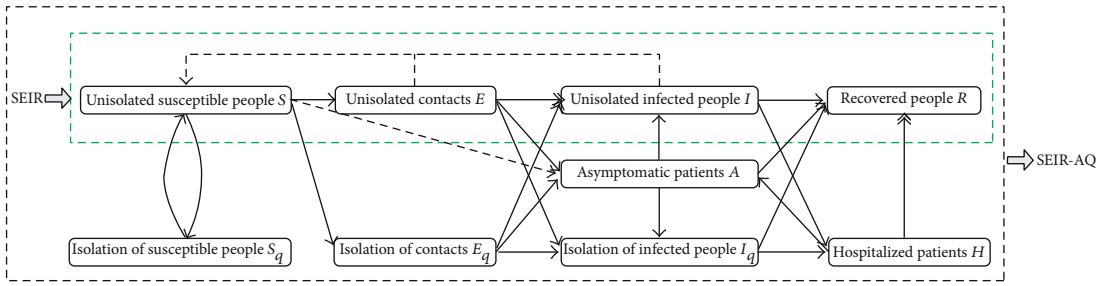

Figure 1: The warehouse conversion relationship of the SEIR-AQ paradigm.

the modified SEIR model established by Cao et al. [17] comprehensively considering the transmission characteristics of COVID-19, the population transformation relationship of SEIR-AQ, which is suitable for analyzing the COVID-19 epidemic situation, is shown in Figure 2. In Figure 2, the gray lines represent the transformation relationship deleted from the original and the red line represents the increased part converted from E_q to H.

At this time, the SEIR-AQ model is

$$\begin{cases} \dfrac{dS}{dt} = -[c\beta + cq(1-\beta)]S(I + \theta A + \upsilon E) + \lambda S_q - \eta S, \\ \dfrac{dE}{dt} = c\beta(1-q)S(I + \theta A + \upsilon E) - (\sigma + \eta)E, \\ \dfrac{dI}{dt} = -(b + r_1 + \alpha + \eta)I + \sigma e E, \\ \dfrac{dA}{dt} = -(r_2 + \eta)A + \sigma(1-e)E, \\ \dfrac{dS_q}{dt} = cq(1-\beta)S(I + \theta A + \upsilon E) - (\lambda + \eta)S_q, \\ \dfrac{dE_q}{dt} = c\beta q S(I + \theta A + \upsilon E) - (\delta + \eta)E_q, \\ \dfrac{dH}{dt} = bI + \delta E_q - (r_4 + \alpha + \eta)H, \\ \dfrac{dR}{dt} = r_1 I + r_2 A + r_4 H - \eta R. \end{cases} \tag{3}$$

The parameter q represents the isolation ratio, β represents the probability of infection, c represents the contact rate, α represents the rate of death due to illness, δ represents the rate where E_q is converted to H, r represents the rate of recovery, e represents the probability that the infected people have symptoms, λ represents the rate of S_q converted to S, θ represents the ratio of the transmission capacity of A compared with I, and η represents the natural mortality rate.

3. Global Stability of the Equilibrium Point

In the proof of this paper, the following equation is considered apart from $R(t)$ [18]:

$$\begin{cases} \dfrac{dS}{dt} = -[c\beta + cq(1-\beta)]S(I + \theta A + \upsilon E) + \lambda S_q - \eta S, \\ \dfrac{dE}{dt} = c\beta(1-q)S(I + \theta A + \upsilon E) - (\sigma + \eta)E, \\ \dfrac{dI}{dt} = -(b + r_1 + \alpha + \eta)I + \sigma e E, \\ \dfrac{dA}{dt} = -(r_2 + \eta)A + \sigma(1-e)E, \\ \dfrac{dS_q}{dt} = cq(1-\beta)S(I + \theta A + \upsilon E) - (\lambda + \eta)S_q, \\ \dfrac{dE_q}{dt} = c\beta q S(I + \theta A + \upsilon E) - (\delta + \eta)E_q, \\ \dfrac{dH}{dt} = bI + \delta E_q - (r_4 + \alpha + \eta)H. \end{cases} \tag{4}$$

According to model (4), we can express $f(I)$ as

$$f(I) = I - \frac{e\sigma\eta(\lambda + \eta)(r_2 + \eta)}{c[\lambda\beta + \eta(\beta + q - \beta q)]\{\sigma e(r_2 + \eta) + [\theta\sigma(1-e) + \upsilon(r_2 + \eta)](b + r_1 + \alpha + \eta)\}}. \tag{5}$$

Then, the derivation with respect to I is computed as

$$f'(I) = 1 > 0. \tag{6}$$

It shows that $f(I)$ is an increasing function as the density of I tends to go infinity, which implies that

$$\lim_{I \to +\infty} f(I) = +\infty. \tag{7}$$

According to equation (5), we can obtain

$$f(0) = -\frac{e\sigma\eta(\lambda+\eta)(r_2+\eta)}{c[\lambda\beta+\eta(\beta+q-\beta q)]\{\sigma e(r_2+\eta)+[\theta\sigma(1-e)+\nu(r_2+\eta)](b+r_1+\alpha+\eta)\}} < 0. \tag{8}$$

So the equilibrium point exists.

$$F = \begin{bmatrix} 0 & 0 & 0 & 0 & \lambda & 0 & 0 \\ c\beta(1-q)(I+\theta A+\nu E) & c\beta(1-q)\nu S & c\beta(1-q)S & c\beta(1-q)\theta S & 0 & 0 & 0 \\ 0 & \sigma e & 0 & 0 & 0 & 0 & 0 \\ 0 & \sigma(1-e) & 0 & 0 & 0 & 0 & 0 \\ cq(1-\beta)(I+\theta A+\nu E) & cq(1-\beta)\nu S & cq(1-\beta)S & cq(1-\beta)\theta S & 0 & 0 & 0 \\ cq\beta(I+\theta A+\nu E) & cq\beta\nu S & cq\beta S & cq\beta\theta S & 0 & 0 & 0 \\ 0 & 0 & b & 0 & 0 & \delta & 0 \end{bmatrix}, \tag{9}$$

$$V = \begin{bmatrix} [c\beta+cq(1-\beta)](I+\theta A+\nu E)+\eta & [c\beta+cq(1-\beta)]\nu S & [c\beta+cq(1-\beta)]S & [c\beta+cq(1-\beta)]\theta S & 0 & 0 & 0 \\ 0 & \sigma+\eta & 0 & 0 & 0 & 0 & 0 \\ 0 & 0 & b=r_1+\alpha+\eta & 0 & 0 & 0 & 0 \\ 0 & 0 & 0 & r_2+\eta & 0 & 0 & 0 \\ 0 & 0 & 0 & 0 & \lambda+\eta & 0 & 0 \\ 0 & 0 & 0 & 0 & 0 & \delta+\eta & 0 \\ 0 & 0 & 0 & 0 & 0 & 0 & r_4+\alpha+\eta \end{bmatrix}, \tag{10}$$

$$R_0 = \rho\left(FV^{-1}\right). \tag{11}$$

R_0 is the basic reproduction number of model (4). Then, there comes Proposition 1.

Proposition 1. *Model (4) admits a disease-free equilibrium $P^0 = (0, 0, 0, 0, 0, 0)$. If $R_0 > 1$, then model (4) admits a unique endemic equilibrium $P^* = (S^*, E^*, I^*, A^*, S_q{}^*, E_q{}^*, H^*)$:*

$$S^* = \frac{(\sigma+\eta)(r_2+\eta)(b+r_1+\alpha+\eta)}{c\beta(1-q)\{\sigma e(r_2+\eta)+[\theta\sigma(1-e)+\nu(r_2+\eta)](b+r_1+\alpha+\eta)\}}, \tag{12}$$

$$E^* = -\frac{\eta(\lambda+\eta)(r_2+\eta)(b+r_1+\alpha+\eta)}{c[\lambda\beta+\eta(\beta+q-\beta q)]\{\sigma e(r_2+\eta)+[\theta\sigma(1-e)+\nu(r_2+\eta)](b+r_1+\alpha+\eta)\}}, \tag{13}$$

$$I^* = \frac{\sigma e\eta(\lambda+\eta)(r_2+\eta)}{c[\lambda\beta+\eta(\beta+q-\beta q)]\{\sigma e(r_2+\eta)+[\theta\sigma(1-e)+\nu(r_2+\eta)](b+r_1+\alpha+\eta)\}}, \tag{14}$$

$$A^* = \frac{\sigma\eta(1-e)(\lambda+\eta)(b+r_1+\alpha+\eta)}{c[\lambda\beta+\eta(\beta+q-\beta q)]\{\sigma e(r_2+\eta)+[\theta\sigma(1-e)+\nu(r_2+\eta)](b+r_1+\alpha+\eta)\}}, \tag{15}$$

$$S_q{}^* = \frac{q\eta(1-\beta)(\sigma+\eta)(r_2+\eta)(b+r_1+\alpha+\eta)}{c\beta(1-q)[\lambda\beta+\eta(\beta+q-\beta q)]\{\sigma e(r_2+\eta)+[\theta\sigma(1-e)+\nu(r_2+\eta)](b+r_1+\alpha+\eta)\}}, \tag{16}$$

$$H^* = \frac{\eta(\lambda+\eta)(r_2+\eta)[b\sigma e(1-q)(\delta+\eta)+\delta q(\sigma+\eta)(b+r_1+\alpha+\eta)]}{c(r_4+\alpha+\eta)(\delta+\eta)(1-q)[\lambda\beta+\eta(\beta+q-\beta q)]\{\sigma e(r_2+\eta)+[\theta\sigma(1-e)+\nu(r_2+\eta)](b+r_1+\alpha+\eta)\}}. \tag{17}$$

Next, the global stabilities of the equilibria of model (4) around the disease-free equilibrium and the endemic equilibrium are investigated in Theorem 2, respectively.

Theorem 2. *If $R_0 \le 1$, then the disease-free equilibrium $P^0 = (0, 0, 0, 0, 0, 0, 0)$ of model (4) is globally asymptotically stable. If $R_0 > 1$, then the unique endemic equilibrium $P^* = (S^*, E^*, I^*, A^*, S_q{}^*, E_q{}^*, H^*)$ of model (4) is globally asymptotically stable.*

4. Model Parameter Assignment and Verification

To further illustrate the applicability of the SEIR-AQ model, we select COVID-19 data from China, America, Brazil, and India for analysis. The numbers of BRIC, China, Brazil, and India share the similar economic level while America boosts higher level. At the same time, China and India have relatively higher population density. America and Brazil have similar populations and prevention and control awareness. Based on the SEIR-AQ model and the values of different parameters, the impact of different prevention and control measures, prevention and control awareness, economic level, and medical level on the development trend of the COVID-19 epidemic is simulated.

4.1. Parameter Setting and Fitting. The initial values of the SEIR-AQ model were referenced to the single-day confirmed data of COVID-19 in four countries from January 23, 2020, to November 10, 2020. The parameters were estimated in conjunction with relevant literature. The initial values are shown in Table 1, and the parameter values are shown in Table 2. The evaluation index of the SEIR-AQ model fit was the coefficient of determination [12], which is shown in Table 3.

From Figure 3, it can be concluded that the number of single-day confirmed cases of the COVID-19 outbreak in China increased rapidly at the beginning of the outbreak, peaked in February 2020, and then decreased rapidly to a stable and manageable state. The COVID-19 outbreak in America started in April and soon reached to top on April 5 and July 20, respectively. The overall trend of single-day confirmed cases continued to increase. Meanwhile, when it comes to Brazil and India, the number continued to decrease after the peak at August 1 and September 26, respectively, and continued to decrease thereafter. The predictions based on the SEIR-AQ model fit basically matched the actual epidemic development trend, and the SEIR-AQ model fitting evaluation index determination coefficient R^2 is greater than 85%, indicating that the SEIR-AQ model has a significant fitting effect and can predict the development trend of the COVID-19 epidemic.

5. Further Discussion of the SEIR-AQ Model

In this paper, we analyze and study COVID-19 based on the SEIR-AQ model, theoretically analyze the law of COVID-19 evolution, and analyze the influence of different countries' prevention and control measures, prevention and control awareness, economic level, and medical level on their COVID-19 evolution, in which the peak number of new confirmed cases in each country when the parameters change is shown in Table 4.

5.1. Assessment of the Impact of Prevention and Control Measures and Prevention and Control Awareness on the COVID-19. Since the emergence of the COVID-19 epidemic, the Chinese government has decisively adopted strict prevention and control measures to reduce c and increase q. Under the positive instructions of the Chinese government, the citizens gradually raise their awareness of epidemic prevention and control, which reduced ρ and minimized the development of clustered epidemics. As a result, the COVID-19 epidemic tends to be in a more controllable and stable state. In the initial period of the COVID-19 outbreak, only few effective prevention and control measures were taken by the United States government. This then lead to large c and small q which finally resulted in a significant increase in the number of the COVID-19 confirmed cases in a single day. Relatively weak awareness of prevention and control among U.S. nationals led to large ρ. Although America strengthened its prevention and control measures in the later period, it had missed the prevention and control window period, which led to the development of the COVID-19 epidemic. In April 2020, the COVID-19 epidemic developed on a large scale in Brazil. The lack of timely adoption of prevention and control measures proposed by WHO indirectly led to lower awareness of prevention and control among the Brazilian population, which increased c and ρ and lowered q. The number of single-day confirmed cases in Brazil continued to hit a record high. But in June, the government introduced compulsory epidemic prevention measures, such as the adoption of entry restrictions. The number of single-day confirmed

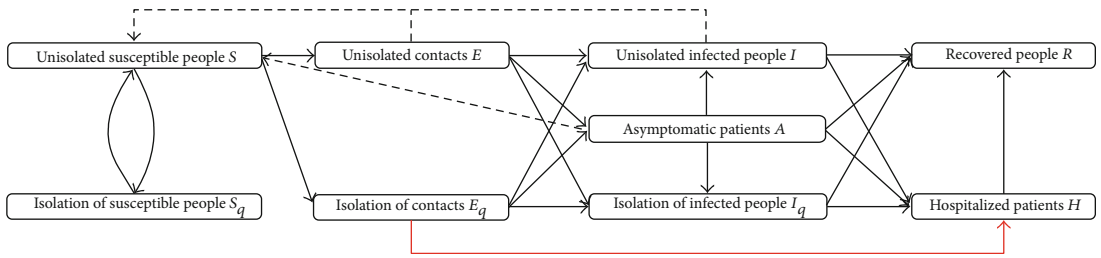

Figure 2: The warehouse conversion relationship of the SEIR-AQ model.

Table 1: SEIR-AQ model initial value setting.

Status	China	India	America	Brazil	Description
S	14×10^8	13.6×10^8	3.28×10^8	2.11×10^8	Total population data
E	4776	4314	5470	3904	Number of single-day confirmed cases
I	524	694	752	647	Official data
R	31	10	15	6	Official data
S_q	2776	1457	2652	1568	Official data, still under medical observation
H	924	854	1213	797	Patient isolation and partial medical observation, $I + E_q$
E_q	400	160	460	150	Estimated value, less than the number of people still under medical observation
A	262	347	376	324	Assuming that the undetected ratio is 0.5, $0.5I$

Table 2: SEIR-AQ model parameter values.

Parameter	China	India	America	Brazil	Description
q	4.98×10^{-10}	3.2×10^{-9}	3.04×10^{-9}	5.6×10^{-9}	Fitting optimization based on actual data
β	1×10^{-8}	0.7×10^{-8}	2.5×10^{-8}	0.5×10^{-7}	Fitting optimization based on actual data
c	2.2	3.8	3.5	3	Fitting optimization based on actual data
σ	1/7	1/7	1/7	1/7	The incubation period is set to 7 days
α	2.7×10^{-4}	4.6×10^{-2}	4.5×10^{-4}	3.4×10^{-2}	Adjusting based on the actual number of deaths
δ	0.13	0.017	0.076	0.03	Fitting optimization based on actual data
$r_1 = r_2 = r_4 = r$	3.5×10^{-2}	2×10^{-4}	3×10^{-6}	1.2×10^{-3}	Adjusting based on the actual number of people recovered
e	0.4	0.37	0.4	0.35	Fitting optimization based on actual data
λ	1/14	1/14	1/14	1/14	The quarantine period is set to 14 days
θ	1	1	1	1	Assuming that the contact is the same as the patient who has shown symptoms
η	0	0	0	0	Assuming that the natural mortality rate is 0

Table 3: Analysis of the fitting degree of the SEIR-AQ model.

	$\bar{y}$	SS_{tot}	SS_{res}	R^2
China	2.3482×10^3	8.6654×10^9	4.9524×10^7	0.9943
America	3.5596×10^4	1.9986×10^8	2.0080×10^7	0.8995
Brazil	2.1719×10^4	8.0718×10^7	6.3786×10^6	0.9210
India	3.0041×10^4	2.8920×10^8	1.6288×10^7	0.9437

cases has gradually decreased since the beginning of August. With only a few hundred cumulative cases, India has adopted prevention and control measures relatively early. Since a city closure policy was implemented on March 25, 2020, the country went into emergency closure. Considering that India boosts a huge population and most of Indians lack enough literacy level and awareness of prevention and control, high-density aggregation of people have caused the virus to spread across the country, resulting in large c, small q, and small ρ, which promotes the outbreak of India's COVID-19. In the theoretical analysis, we simulate the development trend of the COVID-19 epidemic under different prevention and control measures by changing c, q, and ρ, which are used to evaluate the impact of prevention and control measures on the development trend of the COVID-19 epidemic. This is shown in Figures 4–6.

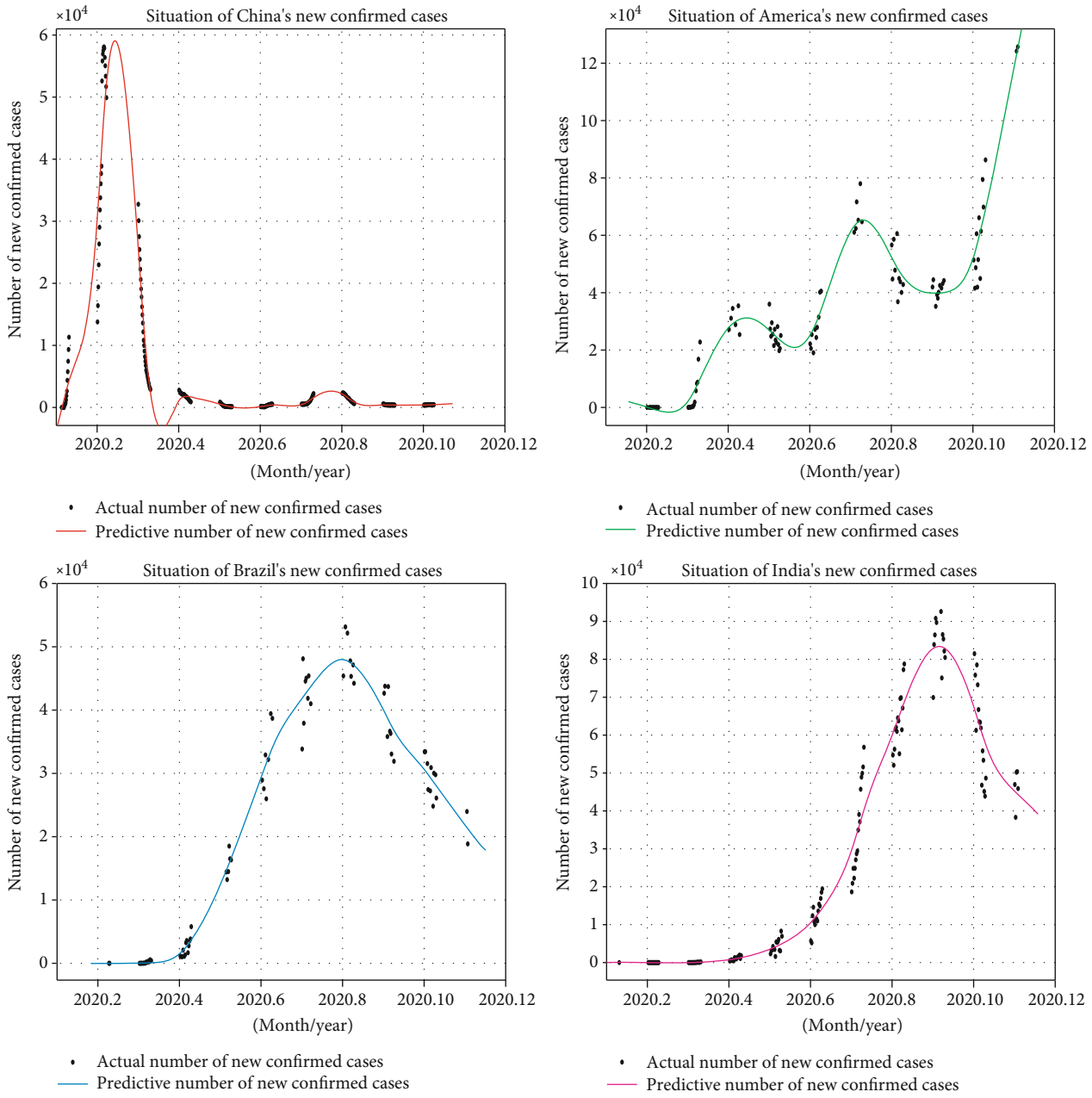

Figure 3: The fitting curve of the number of single-day confirmed cases.

As can be seen from Figure 4,when c is 1.5 times the actual situation in each country, the number of single-day confirmed cases in China will reach a peak of about 7×10^4 in mid-February 2020. In comparison, China reached the earliest and the number of confirmed cases per day tends to be zero at the end of March and remains stable. In America, the number of single-day confirmed cases has continued to increase after reaching 7×10^4. The peak in Brazil has reached about 6×10^4 and then gradually decreased. In India, the number of single-day confirmed cases reached 7×10^4 in August. It will continue to increase to 10×10^4 and then gradually decreased. When comparing the original curve $(1.0q)$ with the different values of the quarantine ratios for each country, it can be observed in Figure 5 that there is a significant delay in the peak number of single-day confirmations at each stage in America, and the peak number of single-day confirmations in the other three countries is correspondingly earlier. The time is correspondingly advanced. As q increases, the peak number of confirmed cases in a single day decreases. When the quarantine ratio of each country is 0.5 times the actual situation, the number of single-day confirmed cases in China will reach a peak of about 7×10^4 in February 2020 and stabilize in March. Around June 2020, the number of confirmed cases in America will reach 7×10^4 and continue to increase to reach the second-stage peak of about 8×10^4. The number of COVID-19 confirmed cases in Brazil and India reached 7×10^4 in a single day in August 2020, respectively, but both will continue to increase

Table 4: Peak number of confirmed countries in a single day when parameters change.

Value	Country	Parameter			
		c	ρ	r	ρ
0.25	China	32830	106160	110060	34530
	America	71140	233740	244150	66090
	Brazil	25570	105510	104060	33650
	India	53750	176190	181270	44490
0.5	China	45540	83200	83480	48340
	America	111020	179980	188650	102090
	Brazil	51580	88320	87040	50550
	India	83570	141810	135300	72440
1.0 (actual peak value)	China	58097	58097	58097	58097
	America	132540	132540	132540	132540
	Brazil	60091	60091	60091	60091
	India	97570	97570	97570	97570
1.5	China	78660	48820	45740	77580
	America	180110	103840	104610	185430
	Brazil	79290	53480	51260	83470
	India	140480	72470	81600	138350
2.0	China	107090	30910	34570	107590
	America	241630	62220	64350	235630
	Brazil	105480	25470	31070	108240
	India	177780	48770	45470	178010

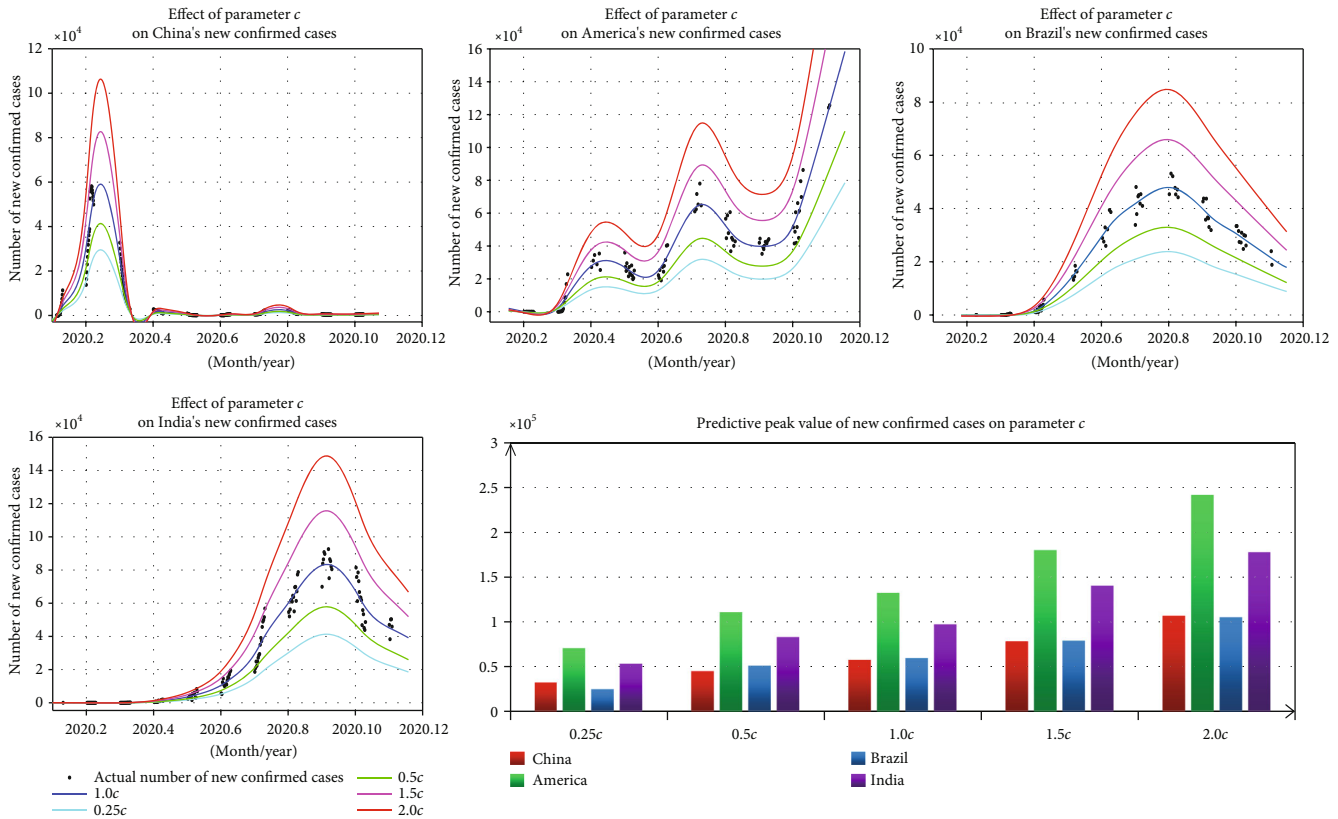

Figure 4: Impact of the contact rate on the COVID-19 outbreak.

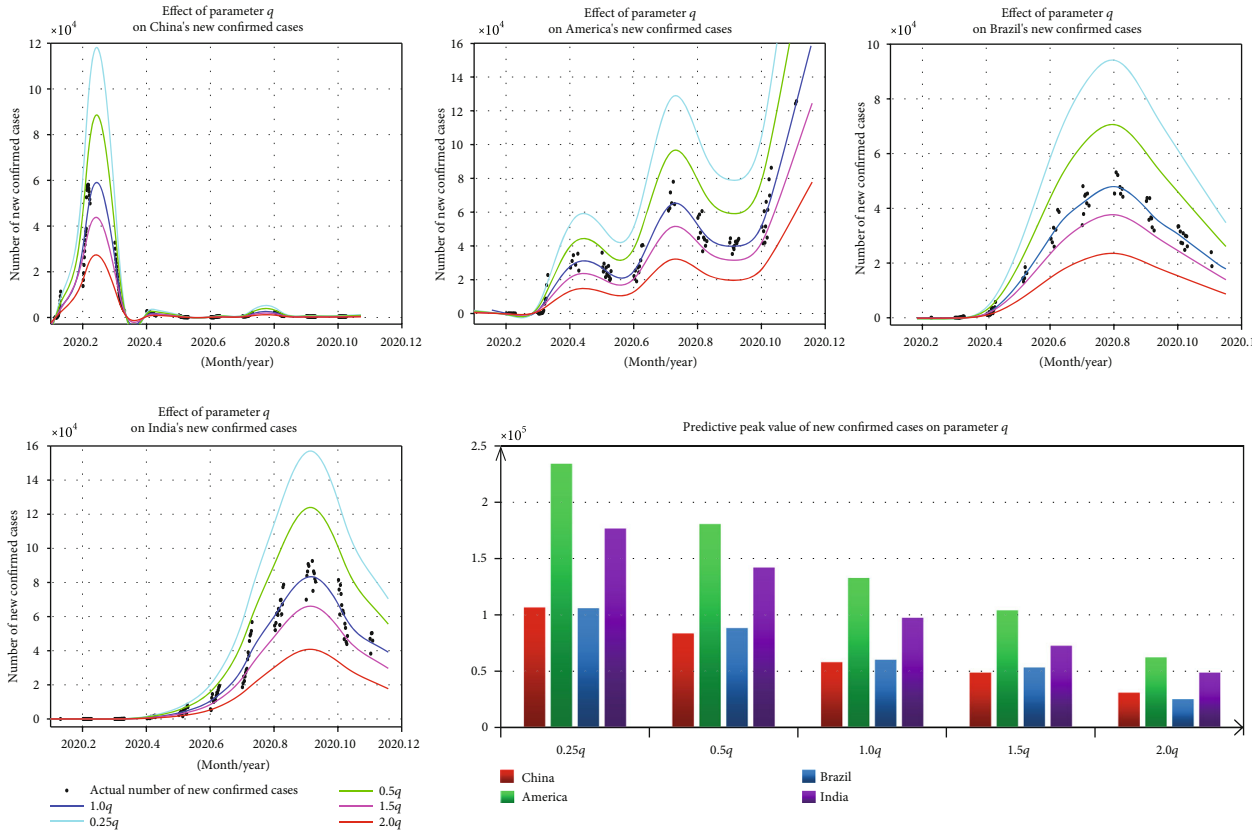

Figure 5: Impact of the quarantine ratio on the COVID-19 epidemic.

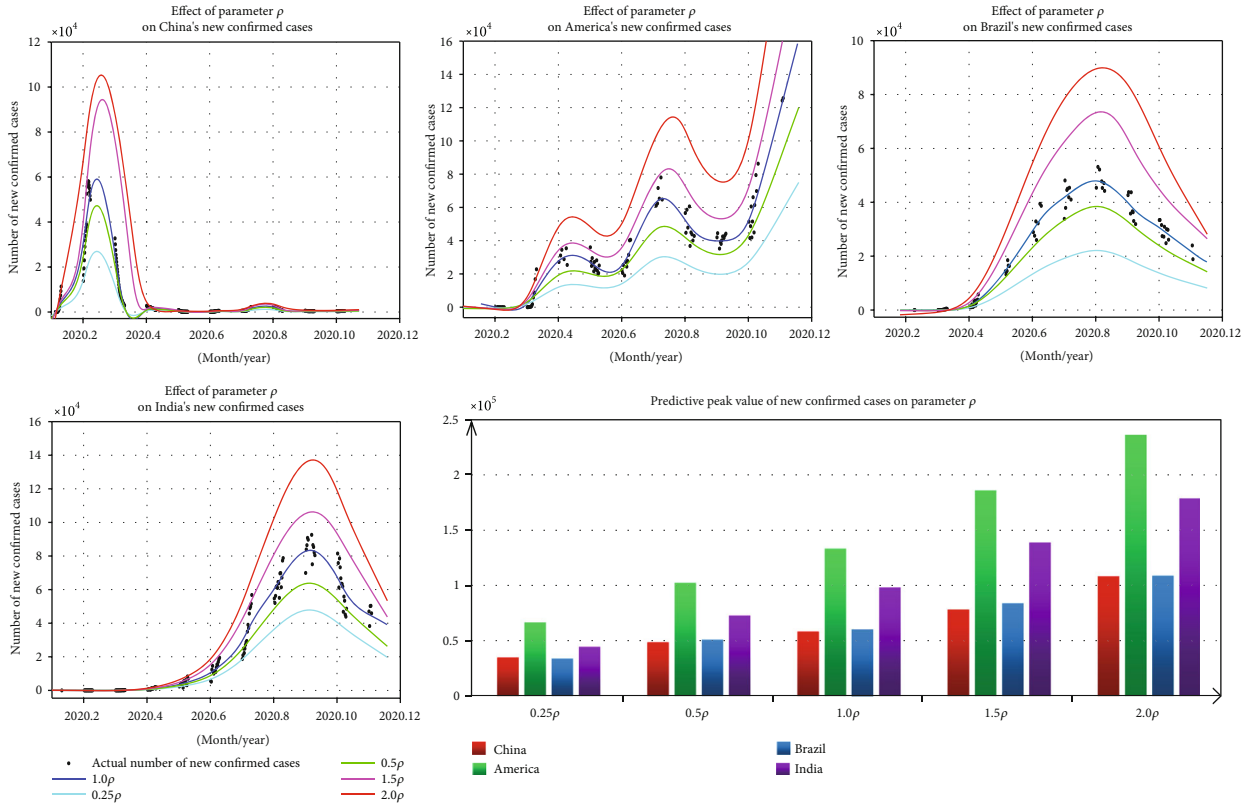

Figure 6: The impact of the effective exposure coefficient on the COVID-19 epidemic.

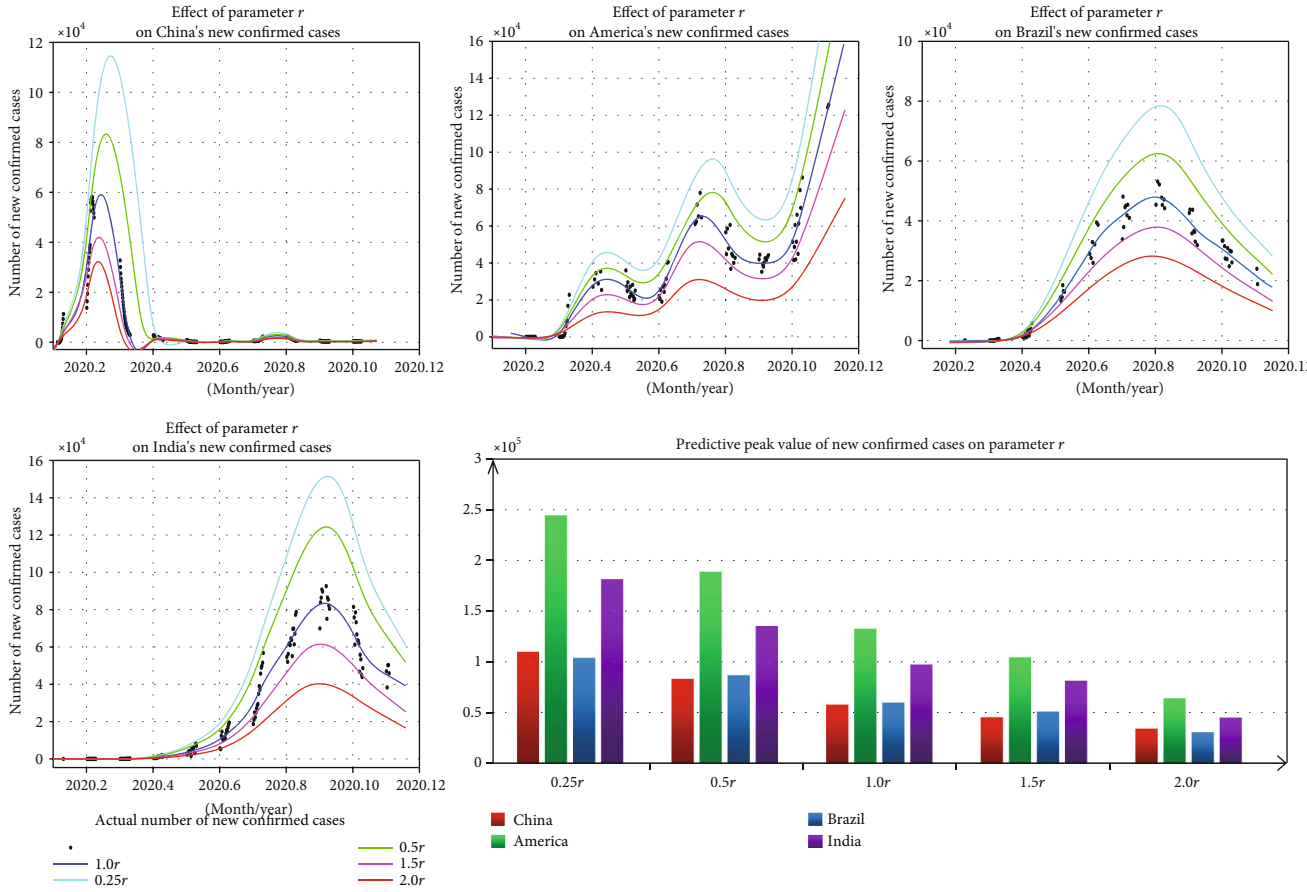

Figure 7: The impact of changes in the recovery rate on COVID-19.

to their respective peaks. According to Figure 6, at ρ of 0.25 times, it takes only one month for the number of confirmed cases in China to reach the highest peak of 3×10^4 in a single day, while it takes only one month for Brazil and India to reach 3×10^4 in mid-to-late July. They need to continue to increase for about a month before reaching their respective peaks. The second-phase peak of the epidemic in America was about 3×10^4. It is expected to continue to increase on a single day.

In China, the government has adopted greater and more rapid prevention and control measures. Chinese people have a strong awareness of prevention and control. So the development of COVID-19 reaches its peak fastest and is rapidly stable. In Brazil and India, the prevention and control measures and people's awareness of prevention and control were relatively weak so that the COVID-19 epidemic reached its peak later. In the United States, the prevention and control measures and people's awareness of prevention and control are weak and continue to increase after reaching the peak of the stage. It indicates that strict and timely prevention and control measures are taken. The higher the awareness of prevention and control, the more effectively the development of the COVID-19 epidemic can be suppressed.

5.2. Assessment of the Impact of Medical and Economic Levels on the COVID-19. As of May 31, 2020, China have allocated a total of ¥162.4 billion in COVID-19 prevention and control at all levels of finance to ensure that financial support for COVID-19 prevention and control measures is in place. After the COVID-19 outbreak, the Chinese government has effectively increased the recovery rate through a large-scale free nucleic acid test, thereby ensuring receiving timely treatment of patients. America invested $8.3 billion in the prevention and control of COVID-19 in the early stage of the COVID-19 outbreak. However, the number of single-day confirmed cases in America reached a peak after April 5, 2020, due to the limited testing capacity. To prevent the collapse of the medical system, the U.S. government adopted restrictions on testing, resulting in low r. Then, the number of single-day confirmed cases fluctuated up and down at the peak. Brazil's uneven distribution of medical resources, insufficient reserves, and a fragile medical system have led to low r, which directly led to the acceleration of the increase in the number of single-day confirmed cases of the COVID-19 epidemic. India's weak basic medical facilities and social medical security system, low virus detection capacity, small size of land area, high population density, and lack of medical equipment have led to the inability to treat infected patients in a timely manner, resulting in low r. This has led to a rapid increase in the number of single-day confirmed cases in June 2020. In the theoretical analysis, we simulate the development trend of the COVID-19 epidemic under different

medical and economic levels by changing r which is used to evaluate the impact of the medical level and economic level on the development trend of the COVID-19 epidemic, as shown in Figure 7.

It can be seen from Figure 7 that under the same scenario (2.0 times the actual r), the COVID-19 epidemic in China will reach a peak of 3×10^4 in early February 2020, with the number of single-day confirmed cases stabilizing around March. The number of single-day confirmed cases in Brazil will reach a peak of about 2.5×10^4 in July 2020 and stabilize after December. The number of single-day confirmed cases of COVID-19 in India will reach 3×10^4 in mid-April and then continue to increase to a peak of 5×10^4. As r in the three countries increases, the time to reach the peak of the number of single-day confirmed cases will be correspondingly advanced and the peak will be correspondingly smaller, with the most significant effect in India. Around July 2020, the number of single-day confirmed cases in America reached 3×10^4, which dropped slightly after reaching the peak of the second phase. However, the number of single-day confirmed cases increased significantly in October.

The Chinese government has invested heavily in the prevention and control of the COVID-19 epidemic and quickly adopted prevention and control measures. The COVID-19 epidemic has stabilized quickly. In Brazil and India, the number of single-day confirmed cases have peaked and stabilized due to fragile medical systems and other reasons. In the United States, although a large amount of money was invested in prevention and control, the uneven distribution of follow-up medical resources has led to a continuous increase in the number of single-day confirmed cases. It shows that increasing capital investment in epidemic prevention and control and sufficient medical resources are conducive to controlling the development trend of the COVID-19 epidemic.

6. Conclusion

In this paper, the transmission dynamic characteristics of COVID-19 are analyzed in four countries based on the SEIR-AQ model: China, America, India, and Brazil. As the economic level, medical level, prevention and control awareness, and prevention and control policies adopted by the four countries China, America, India, and Brazil are significantly different, we fully compare the differences in dynamic parameters such as c, q, r, and ρ among the above four countries and focus on the effects of prevention and control measures, awareness of prevention and control, economic level, and medical level on these parameters. A series of evidence shows that the control of the development of the COVID-19 epidemic requires the local government to quickly take prevention and control measures to minimize the number of exposed people in order to reduce the exposure rate and increase the isolation rate. On this basis, it should also increase financial investment in improving the economic level and medical level to increase the recovery rate, to realize the rapid conversion of confirmed patients to the recovered population. In addition, it is also crucial to raise awareness of prevention and control.

Data Availability

The labeled dataset used to support the findings of this study are available from the corresponding author upon request.

Conflicts of Interest

The authors declare no conflicts of interest.

Acknowledgments

This work is supported by college students' Innovative Entrepreneurial Training Plan Program Grant No. 202010295015Z and the National Natural Science Foundation of China under Grant 61702225.

References

[1] L. Lanjuan and Z. Xueling, "Progress in the prevention and control of the COVID-19," *Zhejiang Medical Journal*, vol. 43, no. 1, pp. 1–8, 2021.

[2] X. Jin, J. S. Lian, J. H. Hu et al., "Epidemiological, clinical and virological characteristics of 74 cases of coronavirus-infected disease 2019 (COVID-19) with gastrointestinal symptoms," *Gut*, vol. 69, no. 6, pp. 1002–1009, 2020.

[3] L. L. R. Du RH, C. Q. Yang, W. Wang et al., "Reply to: Re: predictors of mortality for patients with COVID-19 pneumonia caused by SARSCoV-2: a prospective cohort study," *The European respiratory journal*, vol. 55, 2020.

[4] E. Beretta and Y. Takeuchi, "Global stability of an SIR epidemic model with time delays," *Journal of Mathematical Biology*, vol. 33, no. 3, pp. 250–260, 1995.

[5] K. L. Cooke and P. van den Driessche, "Analysis of an SEIRS epidemic model with two delays," *Journal of Mathematical Biology*, vol. 35, no. 2, pp. 240–260, 1996.

[6] Z. Yu, G. Zhang, Q. Liu, and Q. Lv, "The outbreak assessment and prediction of COVID-19 based on time-varying SIR model," *Journal of University of Electronic Science and Technology of China*, vol. 49, no. 3, pp. 357–361, 2020.

[7] F. Wei, J. Wang, X. Xu et al., "Tendency prediction of COVID-19 worldwide," *Disease Surveillance*, vol. 35, no. 6, pp. 467–472, 2020.

[8] H. Geng, A. Xu, X. Wang, Y. Zhang, X. Yin, and M. A. Mao, "Analysis of the role of current prevention and control measures in the epidemic of corona virus disease 2019 based on SEIR model," *Journal of Jinan University (Natural Science & Medicine Edition)*, vol. 41, no. 2, pp. 175–180, 2020.

[9] W. Guozhu, C. Xiaohang, and Z. Qiang, "Forecast and analysis of epidemic situation based on improved SEIR model," *Journal of Henan Institute of Technology*, vol. 28, pp. 35–39, 2020.

[10] S. Junjie, Y. Shixiong, G. Jingjing, Y. Ming, L. Zhong, and J. Nan, "Comparative analysis of the early transmission characteristics of COVID-19 epidemic between Shandong Province in China and South Korea based on the SEIR model," *Journal of Central China Normal University*, vol. 54, pp. 166–171, 2020.

[11] L. Weiwei, D. Rong, C. Shudong, and S. Shuang, "Analysis of transmission characteristics of COVID-19 and prediction of the development trend of epidemic situation," *Journal of Xiamen University (Natural Science)*, vol. 59, no. 6, pp. 1025–1033, 2020.

[12] J. Lin, "Assessment and prediction of COVID-19 based on SEIR model with undiscovered people," *Journal of University of Electronic Science and Technology of China*, vol. 49, no. 3, pp. 375–382, 2020.

[13] C. Zhenyu, W. Junfen, Q. Kai et al., "Estimation of the COVID-19 epidemic in Italy by an SEAIQR model," *Modern Digestion & Intervention*, vol. 25, no. 3, pp. 273–279+283, 2020.

[14] S. Ansumali, S. Kaushal, A. Kumar, M. K. Prakash, and M. Vidyasagar, "Modelling a pandemic with asymptomatic patients, impact of lockdown and herd immunity, with applications to SARS-CoV-2," *Annual Reviews in Control*, vol. 50, pp. 432–447, 2020.

[15] B. Ivorra, M. R. Ferrández, M. Vela-Pérez, and A. M. Ramos, "Mathematical modeling of the spread of the coronavirus disease 2019 (COVID-19) taking into account the undetected infections. The case of China," *Communications in nonlinear science & numerical simulation*, vol. 88, p. 105303, 2020.

[16] C. Pai, A. Bhaskar, and V. Rawoot, "Investigating the dynamics of COVID-19 pandemic in India under lockdown," *Chaos, solitons, and fractals*, vol. 138, 2020.

[17] S. Cao, P. Feng, and P. Shi, "Study on the epidemic development of COVID-19 in Hubei Province by a modified SEIR model," *Journal of Zhe Jiang University (Medical Sciences)*, vol. 49, no. 2, pp. 178–184, 2020.

[18] J. Jiao, Z. Liu, and S. Cai, "Dynamics of an SEIR model with infectivity in incubation period and homestead-isolation on the susceptible," *Applied Mathematics Letters*, vol. 107, p. 106442, 2020.